Preprint of an article published in:
Chem. Eng. Sci. 63 4789-4799 (2008).

Model-based Determination of Changing Kinetics in High Cell Density Cultures Using Respiration Data

Anja Drews [&,*] and Harvey Arellano-Garcia [§,*]

[§] Department of Process Dynamics and Operation, Sekr. KWT-9

[&] Department of Chemical Engineering, Sekr. MA 5-7

[*]Berlin University of Technology, Str. des 17. Juni 135, D-10623 Berlin, Germany

Abstract

During high-cell-density cultivations very low growth rates and changes in cell metabolism occur. These have to be accounted for in the kinetic modelling. In this work, an optimization-based approach is presented which recognises the switching to new parameters or even to a different model at a certain growth rate and thereby improves the quality of model prediction for different time horizon lengths. For the dynamic automatic adjustment to changing kinetics, a moving horizon estimator (MHE) is used. Experimental data from cultivation of *Ustilago maydis* are used for the model-based parameter identification. To validate the method, initially offline data are used. In the next step, respiration data, which are available online, are used to enable real-time monitoring. The embedded MHE was successfully applied to predict changes in biokinetic constants during membrane bioreactor (MBR) fermentation. Setting suited horizon lengths and parameter bounds was found to be crucial for convergence and parameter estimation. The expected drop in maintenance parameters at low growth rates was confirmed when using an optimum number of data points.

Keywords: biokinetics, fermentation, membrane bioreactor, high cell density, carbon dioxide evolution rate

Preprint of an article published in:
Chem. Eng. Sci. 63 4789-4799 (2008).

Introduction

During high-cell-density cultivations, which are becoming increasingly popular in biotechnology and wastewater treatment, e.g., in membrane bioreactors (MBR), very low growth rates and changes in cell metabolism occur (e.g., Ihssen and Egli, 2004). Due to the rising biomass concentration each cell is subjected to an increasing substrate limitation which leads to a decrease in growth rate down to zero growth. In this region, maintenance metabolism where substrates are used for cell survival instead of growth, and which always takes place in parallel to growth metabolism, gains higher importance. Very low growth rates are often encountered in nature, but the consequences for technical applications have not been described as exhaustively as those at higher growth rates or at starvation conditions (Konopka, 2000). By quorum sensing or stringent response, high cell densities or progressing limitations can also lead to a change in metabolism (e.g. van Verseveld et al., 1984). This means that kinetic parameters determined in common experiments like fed-batch and chemostat do not sufficiently describe conditions, e.g., in MBRs or other high cell density processes. If a change in growth behaviour occurs at low growth rates, a change in production behaviour is of course conceivable (Drews and Kraume, 2005), too, and must be borne in mind when designing a production process. While knowledge on near zero-growth states is scarce it is clear that the emerging phenomena cannot be sufficiently described by kinetic models used during earlier phases in the process when growth rates were higher. Therefore, process monitoring and control requires switching to new parameters or even to a different model at a certain growth rate. Growth rate, however, is a value which cannot be determined directly online.

A model-based identification approach utilising online data is thus needed (Sun et al., 2006). The realisation of such approaches requires, information about the actual state of the processes. It is usually assumed that the state can be gained through measuring essential process variables. In many cases like biotechnological processes, however, it is not possible to measure all

Preprint of an article published in:
Chem. Eng. Sci. 63 4789-4799 (2008).

required variables, especially in on-line applications where a frequent update of measurements is necessary. A broad variety of methods have been proposed to address this problem, ranging from structural or non-structural observability analysis to various kinds of state observers such as the extended Kalman filter. The drawback of these methods lies in the fact that they either give only information about which variables should be additionally measured so as to be able to compute the unmeasured variables (with the method of structural observability analysis) or are only applicable to linear or linearised process models (with the method of state observers). Biotechnological processes, however, are often of a strong non-linear nature. In this work, novel model-based numerical strategies are presented which recognise the switching time and improve the quality of model prediction for different time horizon lengths.

Biokinetic Background

For design, monitoring, and control of a biological process, reliable models are required. Balance equations for the individual components (biomass, nutrients, and metabolites) are coupled via yield coefficients *Y*. These are defined as the rate of change in one concentration over the rate of change in another. Biomass yields from substrate uptake are constant over wide ranges of growth rates. However, especially at very low growth rates, other phenomena must be taken into account. To describe such phenomena, Pirt (1965) introduced the maintenance concept whereby part of the substrate is always used for cell survival and not for reproduction. The corresponding substrate uptake rate (expressed as specific rate $k_{m,S}$) therefore only yields energy for cell maintenance processes. $Y^{g}_{B/S}$ is the so-called true yield which relates the formed biomass *B* to the substrate mass *S* used for growth (superscript *g*) as opposed to maintenance purposes. According to this, the substrate uptake rate can be expressed as:

$$-\dot{r}_S = \frac{\dot{r}_B}{Y^{g}_{B/S}} + k_{m,S} \cdot c_B \qquad (1)$$

Preprint of an article published in:
Chem. Eng. Sci. 63 4789-4799 (2008).

Several other possible mechanisms have been reported (endogenous metabolism, cryptic growth). Whichever phenomenon prevails, a large number of processes can be satisfactorily described by the Pirt concept. It has often been observed and described that $k_{m,S}$ is not constant (Pirt, 1965; Tijhuis et al., 1993). Deviations from the linear relationship between $\dot{r}_s$ and $\dot{r}_B$ seem to occur when growth is limited by a substrate or nutrient other than the energy substrate (Bulthuis et al., 1989; Pirt, 1982). Ihssen and Egli (2004), however, state that the specific growth rate and neither the nature of the limiting nutrient nor cell density is responsible for the relevant stress response. This is in agreement with Drews and Kraume (2007) who observed no significant differences in maintenance parameters for glucose or ammonia limitation. Below $\mu_{crit} \approx 10\ \% \ \mu_{max}$ microorganisms undergo severe changes in metabolism (Van Loosdrecht and Henze, 1999; van Verseveld et al., 1984; Konopka, 2000). Applying the Pirt concept, several authors have reported a significant reduction of maintenance demand at very low growth rates in comparison to chemostat data (Pirt, 1987; Bulthuis et al., 1989; van Verseveld et al., 1984; Low and Chase, 1999; Müller and Babel, 1996; Tros et al., 1996; Drews and Kraume, 2007).

Fig. 1 clearly shows that long-term limited cultures cannot be described by parameters (in this case $k_{m,S}$) determined for short-term limited cultures and early process phases. To overcome this problem, a strategy is required to improve the predictivity of kinetic models. Either the model equation needs to be changed or the parameters need to be set to new values at a certain time or growth rate, respectively. The Pirt concept might not be suited for understanding biochemical processes, but it is widely used and suited for technical applications as long as model parameters are determined in the respective range of operation. Therefore, in this work a switch to new values in the Pirt model is considered.

Preprint of an article published in:
Chem. Eng. Sci. 63 4789-4799 (2008).

Materials and Methods

Ustilago maydis was used as a model organism to determine maintenance parameters. *Ustilago maydis* is a phytopathogenic fungus growing yeast-like in oval shaped single cells (length approx. 10 μm). It can be used for production of ferrichrome, a siderophore with a variety of medical and agricultural applications (Neilands, 1995). *U. maydis* was stored in glycerol stocks (25%) at –80 °C. After a 3-day inoculation on potato-dextrose-agar cells were transferred for approx. 24 h into shaking flasks (100 min^{-1}, 27 °C) containing a defined medium with glucose as the main carbon source. For cultivation, a 5 L glass fermentor (B.Braun Int., Germany) was used (see Fig. 2). In MBR runs, the reactor was equipped with an external ceramic tubular membrane module for biomass retention (Pall Schumacher, Germany). Temperature was controlled at 27 °C, pH at 7.2, and pO_2 at 40 %. To study the effects of glucose and ammonia limitation, respectively, and the effects of short- and long-term limitation, different batch, fed-batch, chemostat and MBR cultivations were carried out (Drews and Kraume, 2007). Biomass concentration was determined by turbidity measurements at 600 nm (UV-120-01, Shimadzu) calibrated against dry weight measurements. Glucose and nutrients concentrations were determined using commercial test kits (liqui-color, Human GmbH, Germany; LCK 303/304, Dr. Lange GmbH, Germany). The concentration of ferrichromes in the supernatant was measured by the CAS-method (Schwyn and Neilands, 1987) whereby unchelated siderophores can be detected. All samples were membrane filtered before analyses. Carbon dioxide in the off-gas was measured using a gas analyser S 710 (Maihak, Germany) with a detection module of type FINOR.

Process Modelling

A model was developed to describe the considered process. The model approach includes mass balances and kinetics (eqs. 2-11), with the kinetic parameters μ_{max}, K_i, Y_i and k_i being subject to possible changes during the fermentation. At the given conditions, the concentrations of

Preprint of an article published in:
Chem. Eng. Sci. 63 4789-4799 (2008).

glucose c_C, ammonia c_N and ferrichrome c_P were identified as the main influencing parameters for growth of *Ustilago maydis*. Thus, the following expression was derived. For glucose, a Monod term was chosen while for ammonia and ferrichrome inhibition was observed at higher concentrations:

$$\mu = \mu_{\max} \cdot \frac{c_C}{c_C + K_{S,C}} \cdot \frac{c_N}{c_N + K_{S,N} + \frac{c_N^2}{K_{I,N}}} \cdot \frac{c_P}{c_P + K_{S,P} + \frac{c_P^2}{K_{I,P}}} \tag{2}$$

with μ_{max} = 0.28 h^{-1}, $K_{S,C}$ = 0.7 g L^{-1}, $K_{S,N}$ = $2 \cdot 10^{-4}$ g L^{-1}, $K_{S,P}$ = $6 \cdot 10^{-3}$ g L^{-1}, $K_{I,N}$ = 1.95 g L^{-1}, and $K_{I,P}$ = 0.115 g L^{-1} (Drews, 2004).

The kinetic parameters specific growth, substrate uptake and production rates depend on different conditions such as substrate and production concentrations, among others. Balance equations for the individual components (biomass, substrates, nutrients, and metabolites) are coupled via yield coefficients *Y*. Especially for low growth rates, maintenance concepts need to be implemented where substrate uptake only yields energy for cell survival. The following set of equations describes the system at constant volume and constant total density:

$$\frac{dm_{total}}{dt} = 0 = \dot{m}_{in} - \dot{m}_{out} \qquad \Rightarrow \qquad \frac{dV_R}{dt} = 0 = \dot{V}_{in} - \dot{V}_{Permeate} - \dot{V}_B \tag{3}$$

$$V_R \cdot \frac{dc_B}{dt} = -\dot{V}_B \cdot c_B + \dot{r}_B \cdot V_R \tag{4}$$

$$V_R \cdot \frac{dc_C}{dt} = \dot{V}_{in} \cdot \left(c_{C,in} - c_C\right) + \dot{r}_S \cdot V_R \tag{5}$$

Preprint of an article published in:
Chem. Eng. Sci. 63 4789-4799 (2008).

$$V_R \cdot \frac{dc_N}{dt} = \dot{V}_{in} \cdot \left(c_{N,in} - c_N \right) + \dot{r}_N \cdot V_R \tag{6}$$

$$V_R \cdot \frac{dc_P}{dt} = -\dot{V}_{in} \cdot c_P + \dot{r}_P \cdot V_R \tag{7}$$

with the

growth rate $\dot{r}_B = \mu \cdot c_B$ (8)

substrate uptake rate $-\dot{r}_S = \frac{\dot{r}_B}{Y^g_{B/S}} + k_{m,S} \cdot c_B$ (9)

ammonia uptake rate $-\dot{r}_N = Y_{N/B} \cdot \dot{r}_B$ (10)

and the production rate $\dot{r}_P = Y^g_{P/B} \cdot \dot{r}_B + k_P \cdot c_B$. (11)

For each time point, the degree of freedom is four. In case of open loop control, the trajectories of the input variables $\dot{V}_{in}$, $\dot{V}_B$, $c_{C,in}$ and $c_{N,in}$ can be used as control or decision variables in an optimisation task (Drews et al., 2006). An inherent characteristic of the MBR process is that a batch phase is required at the beginning when the initial concentrations of the biomass and the possibly, as in this case, inhibitory product are very small, i.e. far from their optimal values. Furthermore, since the volumetric flow rates are set to zero during the batch period, all the other continuous decision variables have no impact on the process either. This is followed by a continuous phase where decision variables have an impact and where concentrations change

Preprint of an article published in:
Chem. Eng. Sci. 63 4789-4799 (2008).

over time until, eventually, the continuous operation reaches a steady state. This makes model based optimisation strategies a challenging task.

The derived model was validated for batch, fed-batch and MBR experiments in Drews (2004). As shown in Fig. 3 and Fig. 4, the experimental and simulation results gives fairly well agreement concerning the trajectories of biomass and ferrichrome concentration during the continuous growth period.

Solution Approach

As stated above, the status of the bioprocess is of crucial importance for its optimisation and control. The presented solution approach is an optimisation-based strategy for parameter estimation that can be used for non-linear systems. A restricted number of past measurements are used to estimate the current state of the system based on the kinetic parameters. These are subject to changes in fermentations with low growth rates. In this section, the moving horizon approach and the parameter estimation (MHE) are addressed. In addition, we propose a formulation for the resulting DAE system that assumes deterministic system behaviour on the estimation horizon. The regulation of the initial values is solved based on a multiple time-scaling discretisation approach.

Multiple time-scaling

Trajectories of the decision variables within a large time horizon need to be computed which requires a discretisation of the time horizon into a large number of time intervals. Due to the rather expected non-monotonous behaviour of state variables within the time intervals (i.e., maxima of glucose and ammonium, and minima of product concentrations) where the feed parameters are constant, the orthogonal collocation method in finite elements (5 collocation

Preprint of an article published in:
Chem. Eng. Sci. 63 4789-4799 (2008).

points) is used as a discretisation approach to guarantee robustness and efficiency at each simulation step (Arellano-Garcia et al., 2005). In addition, a step-size control is integrated to assure convergence at each time interval. By this means, an accurate sensitivity calculation can also be performed which is required for the NLP solver in the optimisation layer. This leads to a novel approach of multiple time-scaling where the step size control (inside one large time interval) is carried out by a 3-layer system (Fig. 5). At the beginning, the step length is first set up in Layer 1, where it is equal to the time interval for the decision variables. In case of convergence, the sensitivities concerning the constraint values at all collocation points are calculated simultaneously. If not, the step size control goes one layer down and so on forth. In Fig. 5, DT or DTs represents the general term for the interval length while the subscripts u and c indicate the correspondence either to the decision interval (ii) or to the interval between the current collocation points, respectively. However, it can also be seen that the end of one interval in Layer 3 is always matched to the next collocation point.

This allows an efficient solution of the following MHE problems and thus the predictivity of cell cultivation is increased as the best fitting class of parameters are used in the DAE model indicating a change in the cell metabolism.

Moving Horizon Estimator

Moving horizon based on-line state estimations have been successfully implemented for several applications (Haseltine and Rawlings, 2005; Rao and Rawlings, 2002) showing an advantage over extended Kalman-filtering because of robustness despite poor initial values and the comfortable use of constraints on state and parameter variables. Considering only recent measurements for the estimation of kinetic parameters, it is possible to recognise values that change during the progress of the estimation time frame.

Preprint of an article published in:
Chem. Eng. Sci. 63 4789-4799 (2008).

The parameter estimation is formulated as an optimisation problem, where the objective function consists of the residuals between the measured values and the result of the model prediction, which is to be minimized. The model equations are formulated as equality and the model restrictions as inequality constraints to the optimisation problem. To estimate the parameters $\boldsymbol{\Theta}$ in the nonlinear implicit equation system, we have several measured data sets of some output (dependent) variables, **y**, and some input (independent) variables **u**. Both **y** and **u** may be subject to measurement errors. In addition, there are some unmeasured state variables in the model, **x**. A general parameter estimation problem with multiple sets of data can be formulated as follows:

$$\min_{\boldsymbol{\Theta},\mathbf{u}_j,\mathbf{x}_j,\mathbf{y}_j} f = \sum_{j=1}^{J} f_j = \sum_{j=1}^{J} \left(\mathbf{y}_j - \hat{\mathbf{y}}_j\right)^T W_Y^{-1} \left(\mathbf{y}_j - \hat{\mathbf{y}}_j\right) + \left(\mathbf{u}_j - \hat{\mathbf{u}}_j\right)^T W_U^{-1} \left(\mathbf{u}_j - \hat{\mathbf{u}}_j\right)$$

s.t.

$$\begin{aligned} &\mathbf{g}_j(\mathbf{x}_j, \mathbf{y}_j, \mathbf{u}_j, \boldsymbol{\Theta}) = \mathbf{0} \quad j = 1, \cdots, J \\ &\mathbf{h}_j(\mathbf{x}_j, \mathbf{y}_j, \mathbf{u}_j, \boldsymbol{\Theta}) \geq \mathbf{0} \\ &\boldsymbol{\Theta}^L \leq \boldsymbol{\Theta} \leq \boldsymbol{\Theta}^U \end{aligned} \tag{12}$$

Where $\mathbf{x} \in X \subseteq \Re^n$, $\mathbf{y} \in Y \subseteq \Re^m$, $\mathbf{u} \in U \subseteq \Re^l$, $\boldsymbol{\Theta} \in \Re^p$, $\mathbf{g} \subseteq \Re^{n+m}$, $\mathbf{h} \subseteq \Re^k$ and W_Y and W_U in the objective function are the known covariance matrixes of the measurement errors of the dependent and independent variables, respectively. $\hat{\mathbf{y}}_j, \hat{\mathbf{u}}_j$ denote the measured values of the dependent and independent variables for data set *j*. **g** is the vector of the model equations and **h** the vector of inequality constraints. The inequality constraints represent process restrictions. The total number of degrees of freedom in this problem is $J \cdot (n+m+l) + p$. However, for large-scale process models the dimension of this optimisation problem can be so large that it cannot be efficiently solved with regular optimisation techniques.

Preprint of an article published in:
Chem. Eng. Sci. 63 4789-4799 (2008).

In this work, a constrained least squares estimation is used to decompose the problem according to the sequential three-stage estimation framework we propose in (Faber et al., 2007), but without estimation of the input variables and assuming no noise or disturbances in the measurements. Therefore, the upper stage solves the actual parameter estimation problem in which the variables **y** and **u** are considered as functions of $\boldsymbol{\Theta}$:

$$\min_{\boldsymbol{\Theta}} f = \sum_{j=1}^{J} f_j = \sum_{j=1}^{J} \left(\mathbf{y}_j(\boldsymbol{\Theta}) - \hat{\mathbf{y}}_j\right)^T W_Y^{-1} \left(\mathbf{y}_j(\boldsymbol{\Theta}) - \hat{\mathbf{y}}_j\right)$$

s.t.

$$\mathbf{g}_j(\mathbf{x}_j, \mathbf{y}_j, \mathbf{u}_j, \boldsymbol{\Theta}) = \mathbf{0}\ ,\ \ j = 1, \cdots, J \tag{13}$$

$$\boldsymbol{\Theta}^L \le \boldsymbol{\Theta} \le \boldsymbol{\Theta}^U$$

The size of this problem is p. In the middle stage, the sub-NLP for each data set are nested in problem (13), where only the independent variables **u** are optimisation variables and thus the size of this problem is l. In the lower stage the measured dependent variables **y** and the unmeasured state variables **x**, representing the largest part of the whole variable space ($n+m$), will be computed by solving the model equations with the Newton algorithm:

$$\mathbf{g}_j(\mathbf{x}_j, \mathbf{y}_j, \mathbf{u}_j, \boldsymbol{\Theta}) = \mathbf{0} \tag{14}$$

This is in fact a simulation step with given $\boldsymbol{\Theta}$ and $\hat{\mathbf{u}}_j$. In order to obtain the sensitivities required for solving the main problem, the gradients of the dependent to the independent variables are required. They can be obtained by using the total differential of the equation system (14) at convergence:

Preprint of an article published in:
Chem. Eng. Sci. 63 4789-4799 (2008).

$$\phi_j(\mathbf{u}_j, \boldsymbol{\Theta}) = \frac{\partial \mathbf{g}_j}{\partial \mathbf{u}_j} + \frac{\partial \mathbf{g}_j}{\partial \tilde{\mathbf{x}}_j} \; \frac{d\tilde{\mathbf{x}}_j}{d\mathbf{u}_j} = \mathbf{0} \tag{15}$$

and thus

$$\frac{d\tilde{\mathbf{x}}_j}{d\mathbf{u}_j} = -\left[\frac{\partial \mathbf{g}_j}{\partial \tilde{\mathbf{x}}_j}\right]^{-1} \frac{\partial \mathbf{g}_j}{\partial \mathbf{u}_j} \tag{16}$$

where $\tilde{\mathbf{x}}_j = [\mathbf{x}_j, \mathbf{y}_j]^T$ and $\frac{\partial \mathbf{g}_j}{\partial \tilde{\mathbf{x}}_j}$, $\frac{\partial \mathbf{g}_j}{\partial \mathbf{u}_j}$ are the Jacobian matrices of the equation system to $\tilde{\mathbf{x}}_j$ and, $\mathbf{u}_j$ respectively. The gradients required for solving problem (13) can be computed by:

$$\frac{df}{d\boldsymbol{\Theta}} = \sum_{j=1}^{J} \frac{\partial f_j}{\partial \mathbf{y}_j} \frac{\partial \mathbf{y}_j}{\partial \boldsymbol{\Theta}} \tag{17}$$

To compute $\frac{\partial \mathbf{y}_j}{\partial \boldsymbol{\Theta}}$, we resort to the model equation system at the convergence according to the multiple time scaling approach proposed above. They can be obtained again by the partial derivatives of equation (14):

$$\frac{\partial \mathbf{g}_j}{\partial \boldsymbol{\Theta}} + \frac{\partial \mathbf{g}_j}{\partial \tilde{\mathbf{x}}_j} \; \frac{\partial \tilde{\mathbf{x}}_j}{\partial \boldsymbol{\Theta}} = \mathbf{0} \tag{18}$$

and then

$$\frac{\partial \tilde{\mathbf{x}}_j}{\partial \boldsymbol{\Theta}} = -\left(\frac{\partial \mathbf{g}_j}{\partial \tilde{\mathbf{x}}_j}\right)^{-1} \frac{\partial \mathbf{g}_j}{\partial \boldsymbol{\Theta}} \tag{19}$$

Preprint of an article published in:
Chem. Eng. Sci. 63 4789-4799 (2008).

The general *moving horizon formulation* follows Robertson et al. (1996) in using a fixed number of recent measurements for the estimation, resulting in a moving time frame that keeps progressing as cultivation time proceeds during the tested experiments.

Results of Kinetic Estimation Based on Offline Data

In this work, experimental data from *Ustilago maydis* cultivations were used for model-based parameter identification and to assess the efficiency of different estimation methods. High cell densities were achieved by using an MBR. Figs. 6 - 8 show the computed biomass, glucose and ferrichrome concentrations for two fed-batch (FB1 und FB2) and two MBR cultivations (MBR1 and MBR2) along with measurements. In general, experimental data are well represented. As can be seen, the extent of deviations from measurements changes with the used horizon length. Local optima seem to exist for the horizon length: For the product concentration in FB1, e.g., the estimation using 8 data points does not lie between the curves for 9 and 7 data points (see also glucose in FB1 and MBR2).

The changing kinetic parameters are plotted in Fig. 9 for FB2 and MBR2. It was expected that maintenance parameters drop as specific growth rate decreases. This is clearly confirmed for MBR2 when using an optimum number of data points for the moving time frame (in this case 10). At approx. 75 h, $k_{m,S}$ abruptly drops from around 0.045 to 0.022 h^{-1} and $Y^{g}_{B/S}$ from 0.55 to 0.3 (see Fig. 10). Using other time frames can cause large overestimations (in this case approx. 50 %). The sensitivity increases with a decreasing number of data points. However, measurements errors can cause large fluctuations here, whereas they get dampened when using more points. It was found that in MBR cultivations the correct value of the maintenance coefficient is more important than that of the true yield (Drews and Kraume, 2007). Hence, optimising the horizon length is of special importance for computing $k_{m,S}$.

Preprint of an article published in:
Chem. Eng. Sci. 63 4789-4799 (2008).

Parameter Estimation using Respiration Rates

Determination of growth, substrate or nutrients uptake and production kinetics normally involves measuring the concentrations of each component which often can only be carried out offline after sampling, and which therefore is a tedious and time-consuming process. Instead, when the required kinetic parameters are known, the carbon dioxide evolution rate can be used for a model-based online estimation of biomass concentration (Lubenova et al., 2003; Drews, 2004; Drews and Kraume, 2007) or, vice versa, for a fit of kinetic parameters. Herbert (1958) already observed a linear relationship between specific carbon dioxide production rate and specific growth rate which was successfully applied to estimate contaminant depletion in soils (Schoefs et al., 2004).

$$\frac{\dot{r}_{CO_2}}{c_B} = Y^g_{CO_2/B} \cdot \mu + m_{CO_2} \tag{20}$$

With eq. (20), integration of the equation for specific growth rate (here with negligible biomass withdrawal),

$$\mu = \frac{1}{c_B}\frac{dc_B}{dt}, \tag{21}$$

leads to the following model equation for the biomass concentration:

$$c_B(t_k + \Delta t) = c_B(t_k)\exp\left[\left(\frac{\dot{r}_{CO_2}}{c_B(t_k)} - k_{m,CO_2}\right)\frac{1}{Y^g_{CO_2/B}} \cdot \Delta t\right] \tag{22}$$

On the lines of this and with the help of a similar expression for the production rate

Preprint of an article published in:
Chem. Eng. Sci. 63 4789-4799 (2008).

$$\dot{r}_P = \frac{Y^g_{P/B}}{Y^g_{CO_2/B}}\left(\dot{r}_{CO_2} - k_{m,CO_2}\right) + \frac{k_P}{Y^g_{CO_2/B}}\int_0^t \left(\dot{r}_{CO_2} - k_{m,CO_2}\cdot c_B\right) dt\,, \tag{23}$$

the produced ferrichrome mass can be formulated as follows:

$$m_P(t_k + \Delta t) = m_P(t_k) + \dot{r}_P \cdot \Delta t \tag{24}$$

Similar to eq. (1), eq. (20) contains a yield coefficient $Y^g_{CO_2/B}$ and a maintenance coefficient k_{m,CO_2}. The substrate taken up for maintenance purposes is solely used for energy production, i.e., it is completely respired and not integrated into biomass or other metabolites. During catabolism, stoichiometric oxidation of 1 mol glucose yields 6 mol CO_2. Using the molecular weights of glucose and CO_2, the maintenance coefficients can thus be converted:

$$k_{m,CO_2} = k_{m,S} \cdot \frac{6 \cdot \tilde{M}_{CO_2}}{\tilde{M}_{Glucose}} \tag{25}$$

From a fit of parameters in Eq. (20) to measured biomass concentrations, maintenance parameters can thus be determined, too. From a comparison of different methods to determine maintenance parameters, it was concluded that a fit of respiration kinetics to biomass concentration is more reliable than plotting a limited number of points from only offline measurements (Drews and Kraume, 2007). It was shown that biomass concentrations can be predicted from CO_2 production over a period of up to 400 hours with a relative deviation of approx. 10 %. To achieve satisfactory fits, different cultivation types (medium or short-term limited as opposed to severely and long-term limited) required distinctly different parameters

Preprint of an article published in:
Chem. Eng. Sci. 63 4789-4799 (2008).

sets. This confirms that parameters indeed change when limitations set in and that progressing parameter estimation is required for reliable process monitoring and control.

In the last section, moving horizon estimation was performed with diverse horizon lengths in order to identify individually changing parameters. Here, with the aim of extending additionally the robustness for a detection of trends in parameter estimates, the optimisation-based strategy for parameter estimation used for non-linear systems is enhanced by a dynamic adjustment of parameter constraints. By this means the estimates of the most recent horizon will form upper and lower bounds for the solution of the optimisation routine in the next calculated horizon. For this purpose, the carbon dioxide evolution rate can be used for a model-based online estimation of biomass concentration. Thus, an optimisation problem is formulated as follows:

$$\begin{aligned} &\min_{\Theta} f = \sum_{i=1}^{I} f_i = \sum_{i=1}^{I} (\mathbf{y}_i - \hat{\mathbf{y}}_i)^T \cdot \mathbf{W} \cdot (\mathbf{y}_i - \hat{\mathbf{y}}_i) \\ &s.t. \\ &\qquad \boldsymbol{\Theta}^L \le \boldsymbol{\Theta} \le \boldsymbol{\Theta}^U \end{aligned} \tag{26}$$

with the constraints on the parameters shown in equation (26) as decision variables, which are now dynamically adapted by the estimates from the previous horizons. A standard NLP-solver (SQP) is used. In this case, the required gradients are approximated with finite difference quotients and not with analytical gradients. The residuals were generated by comparing offline measured biomass and product concentration with the solution of model equations (22) and (24).

Fig. 11 shows the comparison of the model results for the MBR cultivations with the experiment data. In MBR1 a larger fraction of the reactor content was withdrawn at a certain point during the cultivation. Hence, a new starting value was set for biomass modelling which

is why all curves ‘‘merge’’ at one point. Fig. 12 shows the results for parameter estimates corresponding to experiment MBR1 with different horizon lengths and a fixed maximum change of +/- 7% to the last estimate of the global constraint range. For the selected horizon lengths greater dependencies on the number of points are only found for the simulated product concentration for the cultivation experiment after more than 200 hours.

The kinetic parameters for modelling of the biomass concentration (Fig. 12, top) show an explicit evolution over the cultivation time, which seems to be robust against different horizon lengths, when using a fixed maximum parameter change. For the kinetic parameters describing product formation (Fig. 12, bottom), stable trends cannot be verified, but seem to show a decrease for the largest horizon length displayed. In particular, the specific rate for CO_2-respiration, production rate and the yield coefficient for production show different initial estimates in the first calculated horizon, but converge to similar values after approx. 5 horizon estimations. This may be interpreted as a verification of the estimated parameters.

Since the parameter estimation based on respiration data is much faster than solving the complete DAE model, it is suited for real-time online identification of switching points to new parameters. Once these are identified, the rigorous DAE can be computed.

Concluding Remarks

The developed approach for MHE method was succesfully applied to predict changes in kinetic parameters at very low growth rates in an MBR process. Especially when using offline data, setting suited horizon lengths and parameter bounds was found to be crucial for convergence and parameter estimation. The expected drop in maintenance parameters at low growth rates was confirmed when using an optimum number of data points. It is stressed that a drop in

Preprint of an article published in:
Chem. Eng. Sci. 63 4789-4799 (2008).

maintenance demand and possibly a change in production behaviour must be borne in mind when modelling and designing an MBR process.

Nomenclature

c	concentration	[g L^{-1}]
K	half-saturation constant	[g L^{-1}]
k	kinetic coefficient	[h^{-1}]
m	mass	[g]
$\tilde{M}$	molar mass	[g mol^{-1}]
$\dot{r}$	rate of reaction	[g L^{-1} h^{-1}]
t	time	[h]
V	volume	[m^3]
$\dot{V}$	volumetric flow rate	[L h^{-1}]
Y	yield coefficient	[g g^{-1}]
μ	specific growth rate	[h^{-1}]
σ	specific substrate uptake rate	[h^{-1}]

Subscripts and superscripts

B	biomass
C	carbon source (glucose)
in	in
i	component
g	growth
k	iteration step
m	maintenance
out	out

Preprint of an article published in:
Chem. Eng. Sci. 63 4789-4799 (2008).

S	saturation *or* substrate (carbon source)

Abreviations

DAE	differential-algebraic equations
FB	fed batch
MBR	membrane bioreactor
MHE	moving horizon estimator
NLP	non-linear programming

References

Arellano-Garcia, H., Barz, T., Wozny, G., 2007. Close-Loop Stochastic Dynamic Optimization under Probabilistic Output-Constraints. "Assessment and Future Directions of Nonlinear Model Predictive Control", Springer Lecture Notes in Control and Information Sciences Series (LNCIS), in press.

Bulthuis, B.A., Koningstein, G.M., Stouthamer, A.H., van Verseveld, H.W., 1989. A comparison between aerobic growth of *Bacillus licheniformis* in continuous culture and partial-recycling fermentor, with contributions to the discussion on maintenance energy demand. Archives of Microbiology 152, 499-507.

Drews, A., Kraume, M., 2007. On Maintenance Models in Severely and Long-Term Limited Membrane Bioreactor Cultivations. Biotechnology and Bioengineering 96(5), 892-903.

Drews, A., Arellano-Garcia, H., Wendt, M., Kraume, M., Wozny, G., 2006. Optimization of Operating Conditions for Ferrichrome Production in a Membrane Bioreactor Using *Ustilago maydis*. Computer-Aided Chemical Engineering 21A (Eds.: Marquardt, W. Pantelides, C.), 309-314.

Drews, A., Kraume, M., 2005. Process Improvement by Application of Membrane Bioreactors. Trans IChemE, Chemical Engineering Research and Design 83(A3), 276-284.

Drews, A., 2004. Kontinuierliche Ferrichromproduktion mit *Ustilago maydis* im Membranbioreaktor. PhD thesis TU Berlin. Fortschr.-Ber. VDI Reihe 17 Nr. 246, VDI-Verlag, Düsseldorf.

Faber, R., Arellano-Garcia, H., Wozny, G., 2007. An Optimization Framework for Parameter Estimation of Large-Scale Systems. Chemical and Process Engineering, in press.

Haseltine, E. L., Rawlings, J. B., 2005. Critical Evaluation of Extended Kalman Filtering and Moving-Horizon Estimation, Industrial & Engineering Chemistry Research 44, 2451-2460.

Herbert, D., 1958. Some principles of continuous culture. Recent Progress in Microbiology 381-396.

Ihssen, J., Egli, T., 2004. Specific growth rate and not cell density controls the general stress response in *Escherichia coli*. Microbiology 150, 1637-1648.

Konopka, A., 2000. Microbial physiological state at low growth rate in natural and engineered ecosystems. Current Opinion in Microbiology 3, 244-247.

Low, E.W., Chase, H.A., 1999. The effect of maintenance energy requirements on biomass production during waste water treatment. Water Research 33 (3), 847-853.

Lubenova, V., Rocha, I., Ferreira, E.C., 2003. Estimation of multiple biomass growth rates and biomass concentration in a class of bioprocesses. Bioprocess and Biosystems Engineering 25, 395-406.

Müller, R.H., Babel, W., 1996. Measurement of Growth at Very Low Rates ($\mu \geq 0$), an Approach to Study the Energy Requirement for the Survival of *Alcaligenes eutrophus* JMP 134. Applied and Environmental Microbiology 62, 147-151.

Neilands, J.B., 1995. Siderophores: Structure and Function of Microbial Transport Compounds. Journal of Biological Chemistry 270, 26723-26726.

Pirt, S.J., 1965. The maintenance energy of bacteria in growing cultures. Proc. Of the Royal Society of London 163 B, 224-231.

Pirt, S.J., 1982. Maintenance Energy: a General Model for Energy-Limited and Energy-Sufficient Growth. Archives of Microbiology 133, 300-302.

Rao, C. V., Rawlings, J. B., 2002. Constrained process monitoring: moving horizon approach. AIChE Journal, 48, 97-109.

Robertson, D. G., Lee, J. H. ,Rawlings, J. B., 1996. A Moving Horizon Based Approach for Least-Squares Estimation, AIChE Journal 42(8), 2209-2224.

Schoefs, O., Perrier, M., Samson, R., 2004. Estimation of contaminant depletion in unsaturated soils using a reduced-order biodegradation model and carbon dioxide measurement. Applied Microbiology and Biotechnology 64, 53-61.

Sun, Z., Ramsay, J.A., Guay, M., Ramsay, B.A., 2006. Automated feeding strategies for high cell density fed-batch cultivation of *Pseudomonas putida* KT2440. Applied Microbiology and Biotechnology 71, 423-431.

Tijhuis, L., Van Loosdrecht, M.C.M., Heijnen, J.J., 1993. A thermodynamically based correlation for maintenance Gibbs energy requirements in aerobic and anaerobic chemotrophic growth. Biotechnology and Bioengineering 42, 509-519.

Tros, M.E., Bosma, T.N.P., Schraa, G., Zehnder, A.J.B., 1996. Measurement of Minimum Substrate Concentration (S_{min}) in a Recycling Fermentor and Its Prediction from the Kinetic Parameters of *Pseudomonas sp*. Strain B13 from Batch and Chemostat Cultures. Applied and Environmental Microbiology 62, 3655-3661.

Van Loosdrecht, M.C.M., Henze, M., 1999. Maintenance, endogeneous respiration, lysis, decay and predation. Water Science and Technology 39, 107-117.

van Verseveld, H.W., Chesbro, W.R., Braster, M., Stouthamer, A.H., 1984. Eubacteria have 3 growth modes keyed to nutrient flow. Archives of Microbiolology 137, 176-184.

Preprint of an article published in:
Chem. Eng. Sci. 63 4789-4799 (2008).

Fig. 1. Model-based prediction of biomass concentration in short-term (fed-batch) and long-term (MBR) limited cultures (Drews and Kraume, 2005).

Fig. 2. Experimental set-up (MBR flow sheet).

Fig. 3. Biomass concentration in the continuous growth period.

Fig. 4. Ferrichrome concentration in the continuous growth period.

Fig. 5. Layer system for the multiple time scaling

Fig. 6: Ammonium-limited fed-batch experiment FB1 (—: 9, - · -: 8, · · · · ·: 7 data points).

Fig. 7: Glucose-limited fed-batch experiment FB2 (—: 30, - · -: 20, · · · · ·: 10 data points)

Fig. 8: Continuous cultivation experiment MBR1 (—: 8, - · -: 7, · · · · ·: 6 data points).

Fig. 9: Continuous cultivation experiment MBR2 (—: 10, - · -: 8, · · · · ·: 6 data points).

Fig. 10: Parameters estimated for FB2 (top, o: 10, x: 15, +: 20) and MBR2 (bottom, o: 8, x: 9, +: 10 data points).

Fig. 11. Continuous cultivation experiment MBR1 simulated with estimates using a +/- 7% changing rate between single estimation-horizons.

Fig. 12. Parameter estimates corresponding to continuous cultivation MBR1, calculated with a +/- 7% changing rate between single estimation-horizons (Parameter estimates: x: 6, +: 7, o: 8 data points).

Figure

Preprint of an article published in:
Chem. Eng. Sci. 63 4789-4799 (2008).

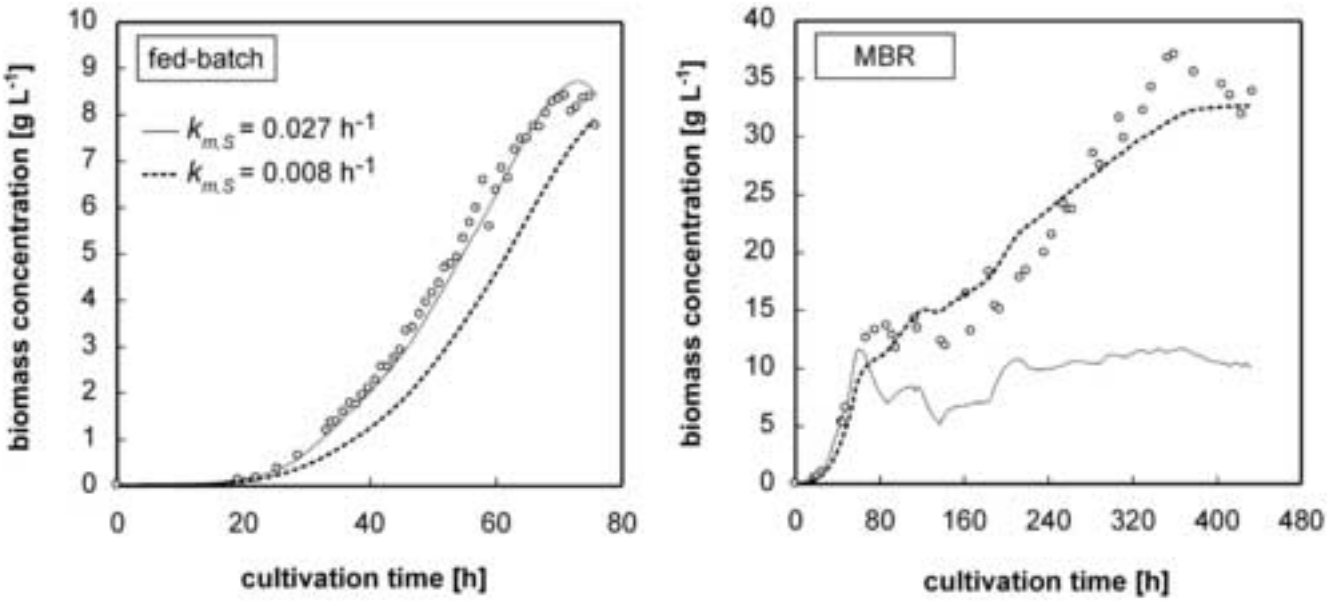

Figure

Preprint of an article published in:
Chem. Eng. Sci. 63 4789-4799 (2008).

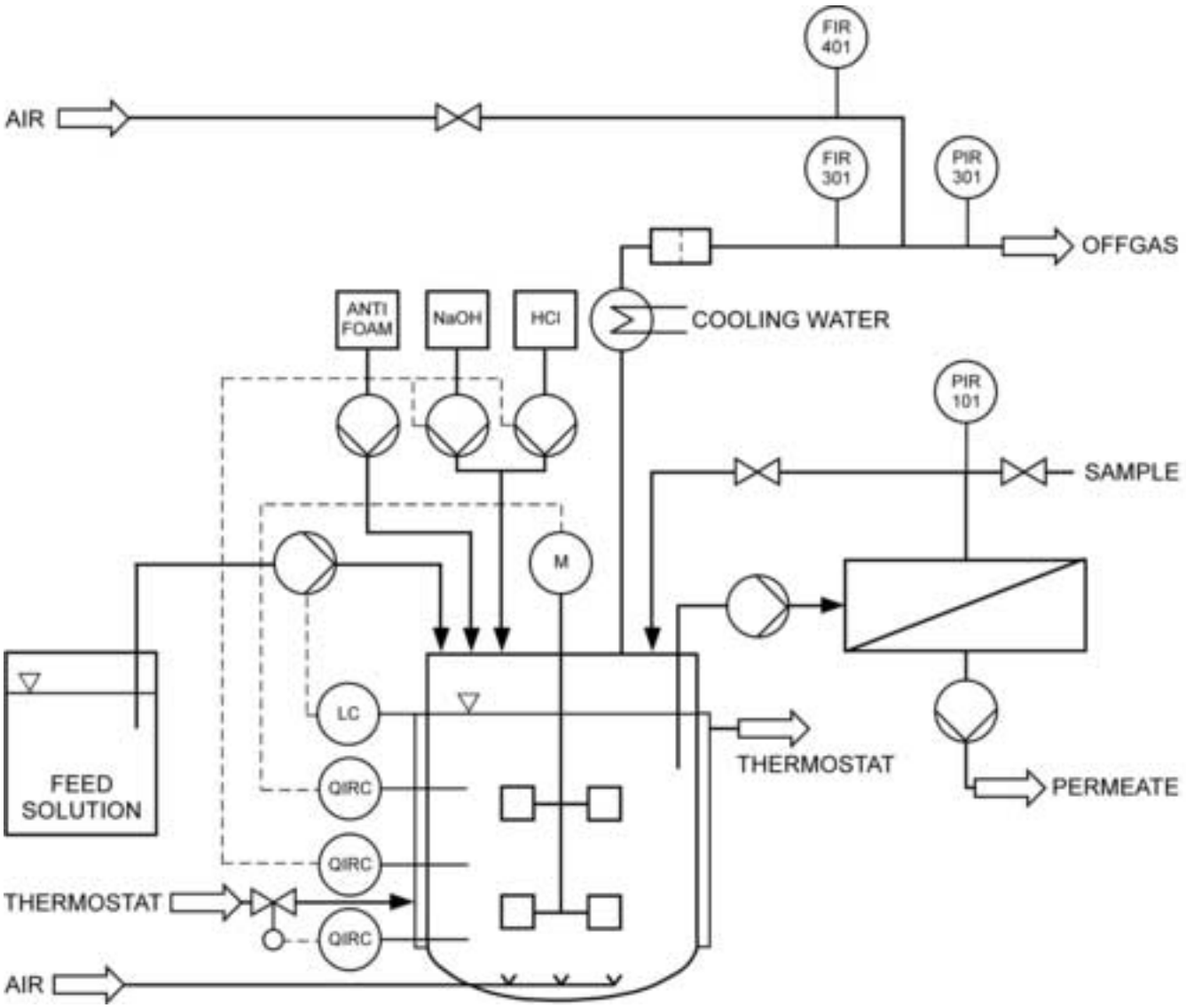

Figure

Preprint of an article published in:
Chem. Eng. Sci. 63 4789-4799 (2008).

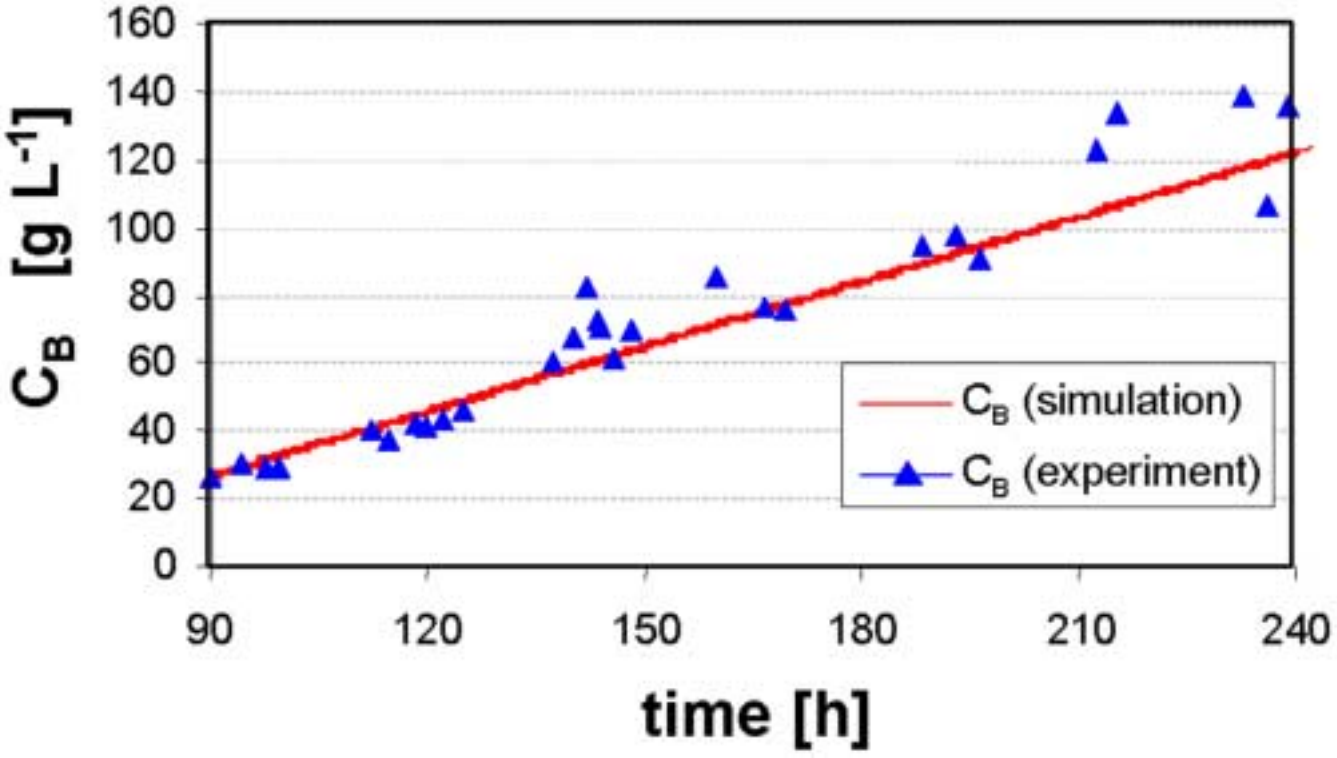

Figure

Preprint of an article published in:
Chem. Eng. Sci. 63 4789-4799 (2008).

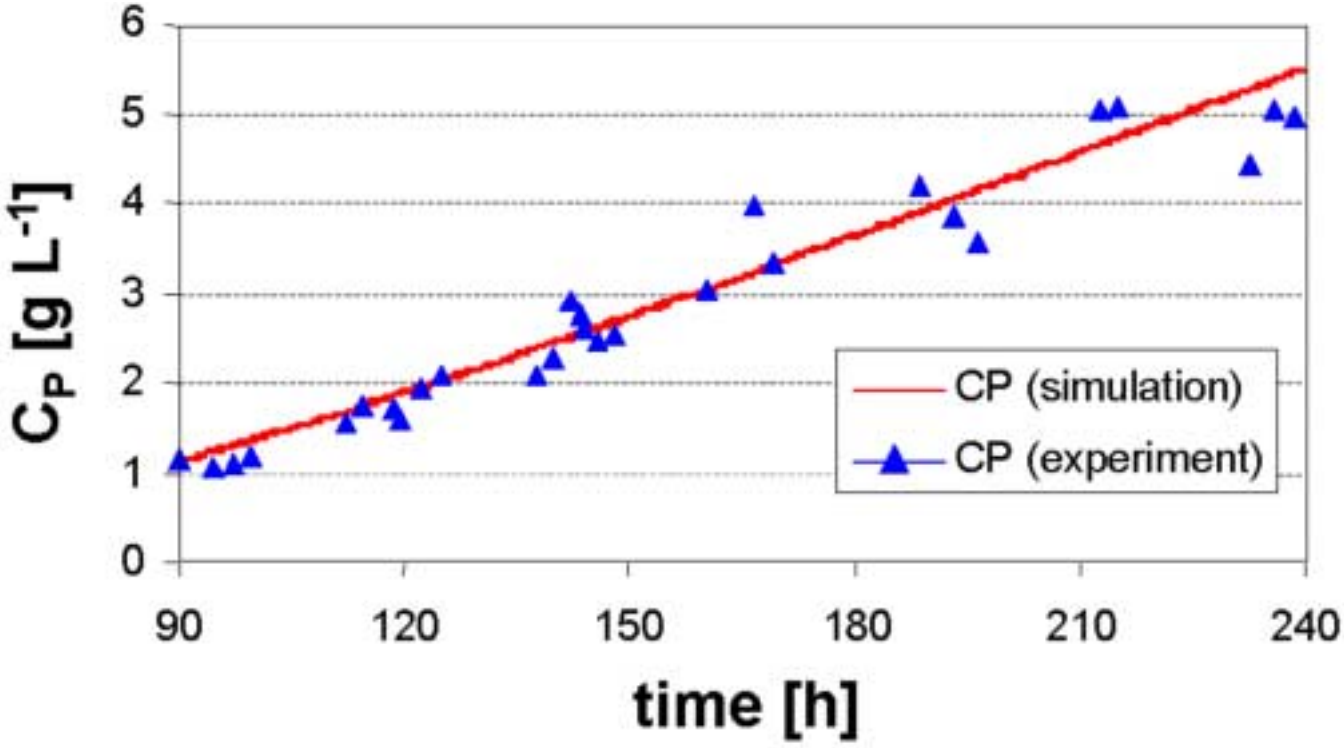

Figure

Preprint of an article published in:
Chem. Eng. Sci. 63 4789-4799 (2008).

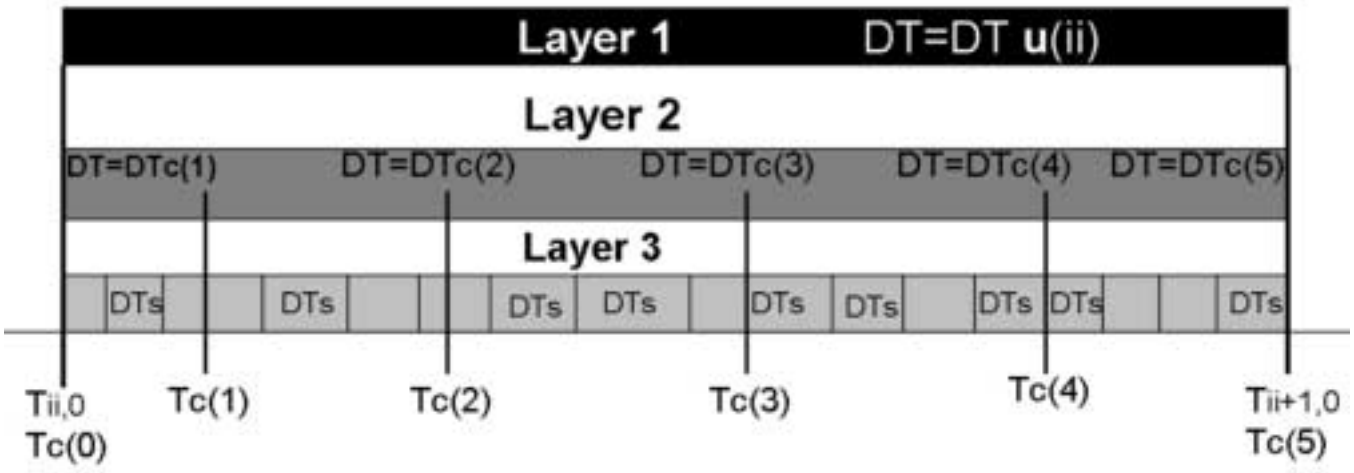

Figure

Preprint of an article published in:
Chem. Eng. Sci. 63 4789-4799 (2008).

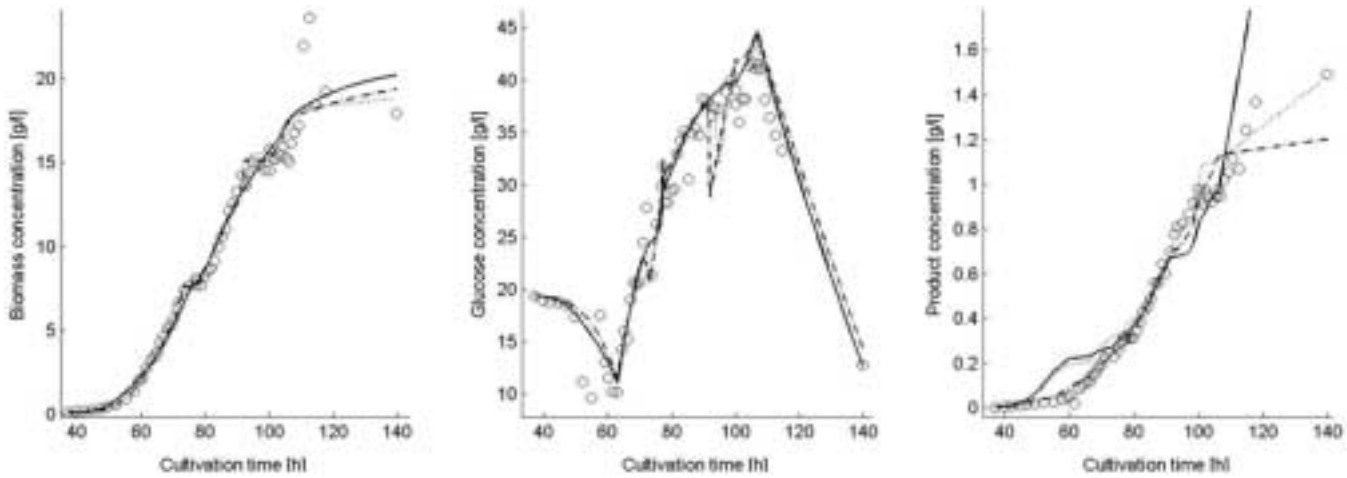

Figure

Preprint of an article published in:
Chem. Eng. Sci. 63 4789-4799 (2008).

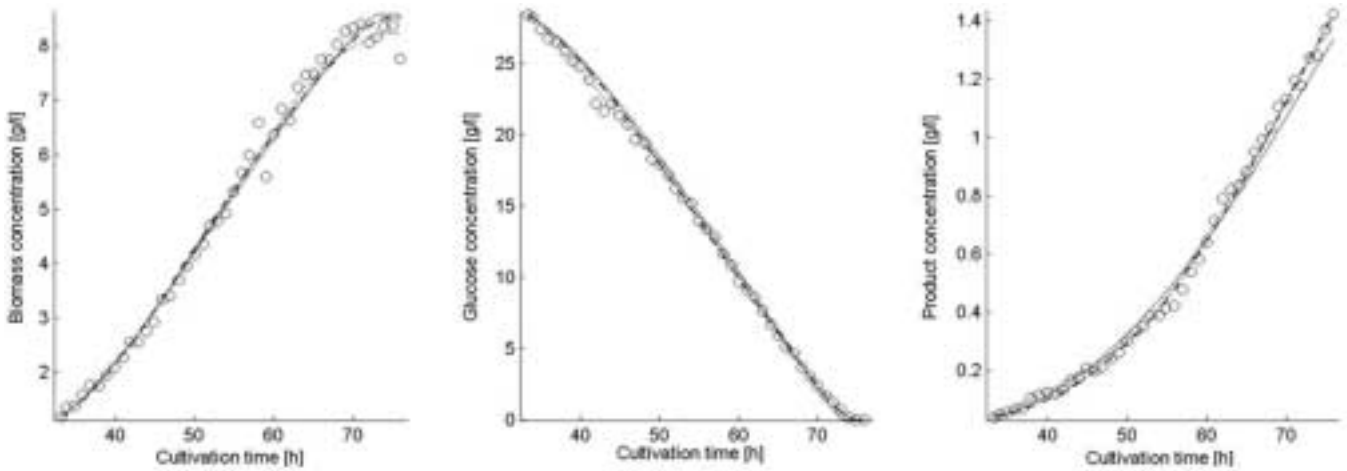

Figure

Preprint of an article published in:
Chem. Eng. Sci. 63 4789-4799 (2008).

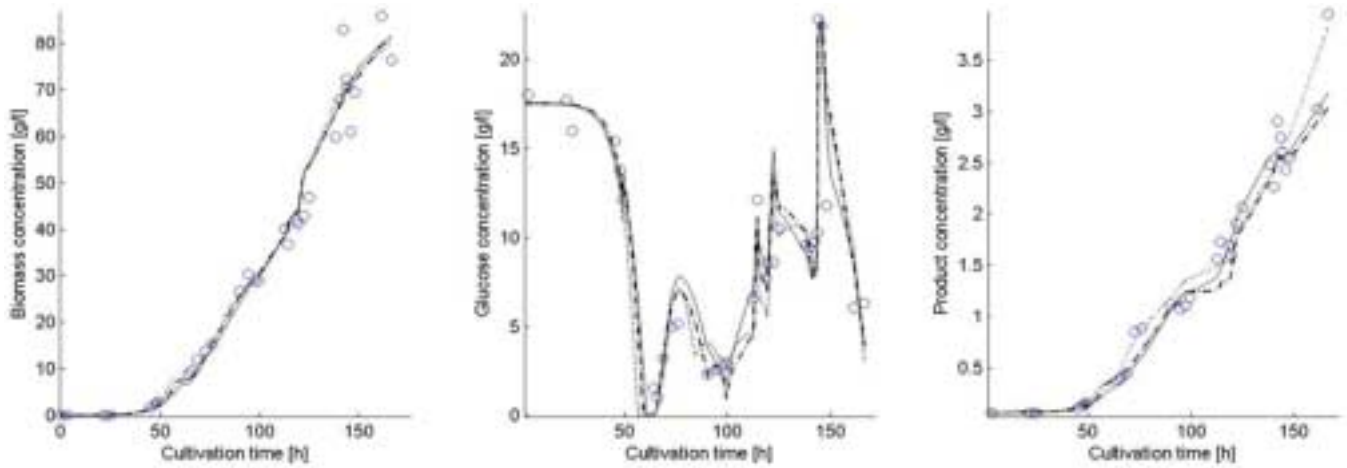

Figure

Preprint of an article published in:
Chem. Eng. Sci. 63 4789-4799 (2008).

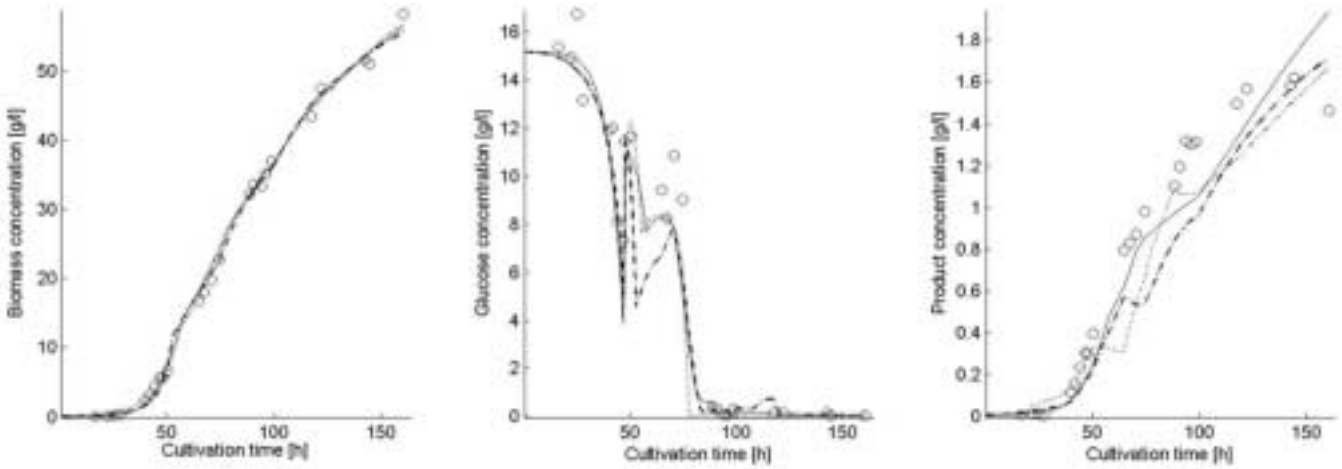

Figure

Preprint of an article published in:
Chem. Eng. Sci. 63 4789-4799 (2008).

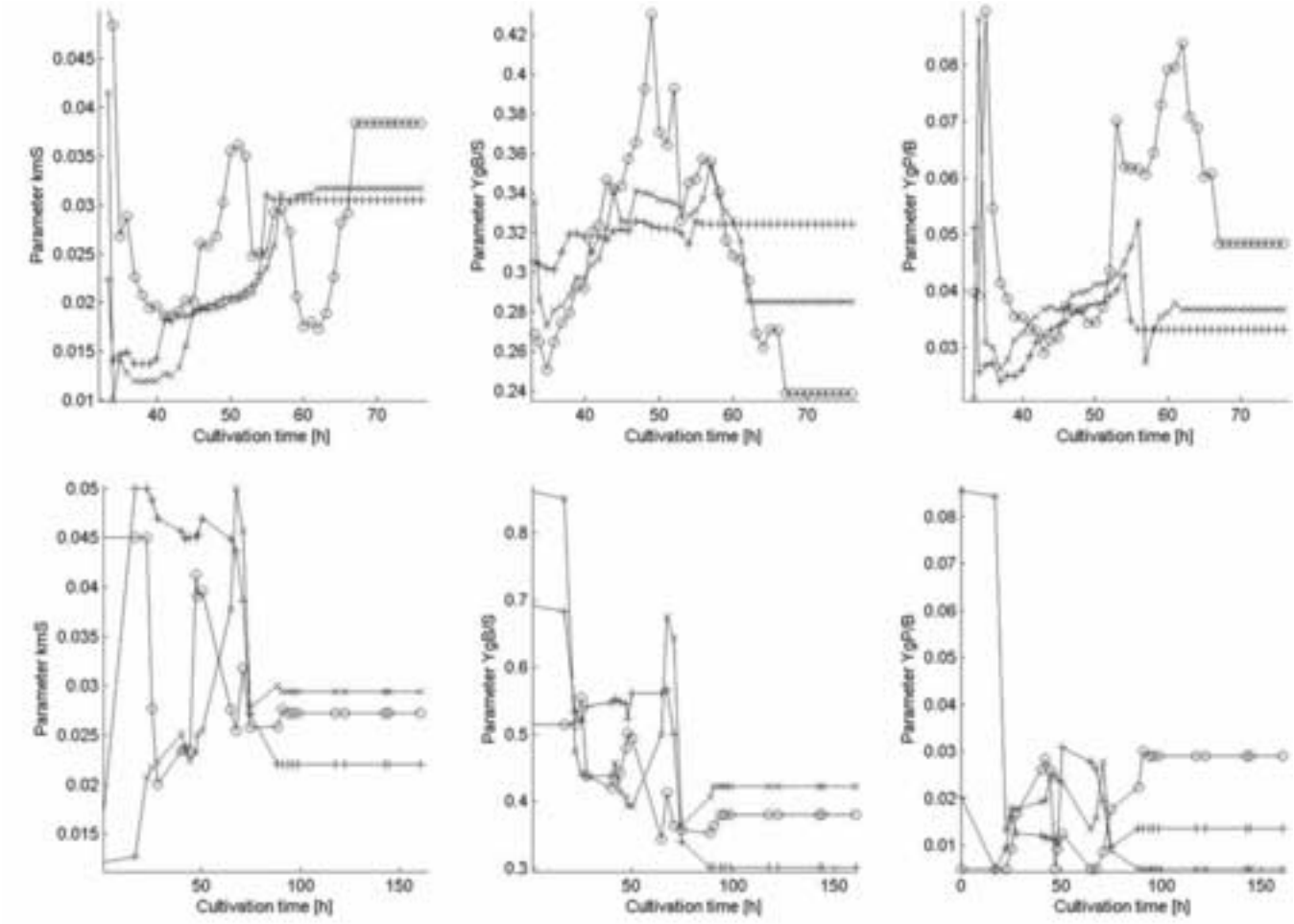

Figure

Preprint of an article published in:
Chem. Eng. Sci. 63 4789-4799 (2008).

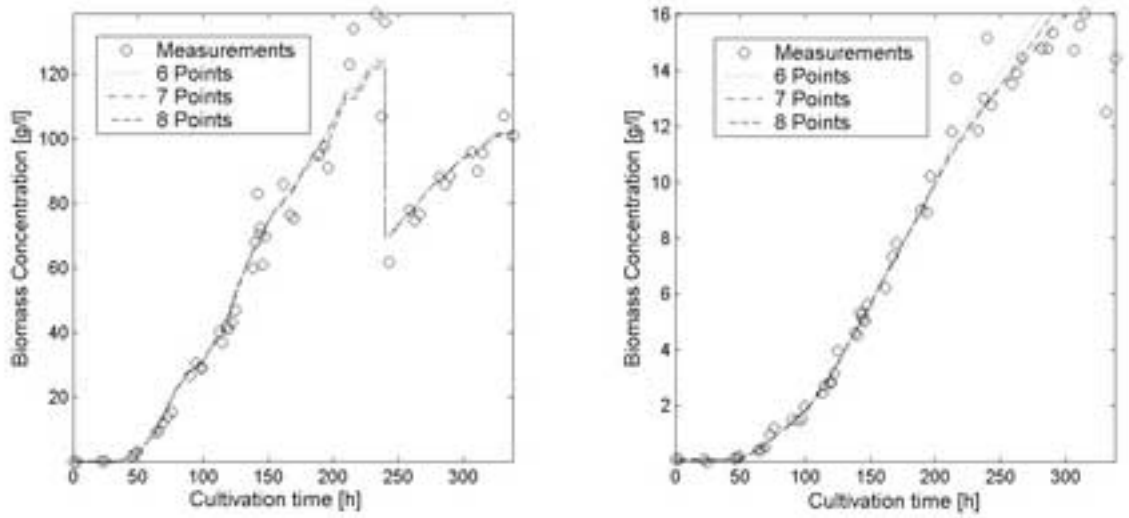

Preprint of an article published in:
Chem. Eng. Sci. 63 4789-4799 (2008).